Preprints of the 19th World Congress
The International Federation of Automatic Control
Cape Town, South Africa. August 24-29, 2014

Data-based Fault Identification and Accommodation in the Control of Sampled-Data Particulate Processes

Trina G. Napasindayao and Nael H. El-Farra

* *Department of Chemical Engineering & Materials Science, University of California, Davis, CA 95616 USA (e-mail: nhelfarra@ucdavis.edu)*

Abstract: This study deals with the problem of actuator fault identification and accommodation in particulate processes with discretely sampled measurements. The methodology involves reducing the infinite-dimensional system describing the particulate process to obtain a finite-dimensional model that captures the process dominant dynamics. A state feedback controller is designed based on the reduced-order model, and a zero-order hold, inter-sample model predictor is used to compensate for the discrete availability of measurements. The inter-sample model predictor is updated at each sampling time once the actual measurements become available. The location and magnitude of the actuator faults are estimated at each sampling time by solving a moving-horizon least-squares optimization problem online. The closed-loop stability properties of the sampled-data system are explicitly characterized in terms of the sampling period, the controller design parameters, and the actuator effectiveness (absence or extent of malfunction), which are subsequently used in the fault accommodation approach that maintains closed-loop stability after a fault occurs. The ability of the proposed methodology to identify and handle simultaneous and consecutive, as well as full and partial faults, are illustrated using a simulated model of a non-isothermal continuous crystallizer.

Keywords: Sampled-data control, fault-tolerant control, fault identification, actuator faults, particulate processes

1. INTRODUCTION

Fault-tolerant control of particulate processes is a fundamental problem encountered in a wide range of industries, including the agricultural, chemical, food, mineral, and pharmaceutical industries. This problem is significant given that malfunctions in the control system or process equipment can negatively impact the particle size distribution of interest and thus harm the desired end product quality. This topic has received limited attention in the process control literature despite the significant research work on the synthesis and implementation of feedback control systems on particulate processes (e.g., see Semino and Ray (1995); Hu et al. (2005); Christofides (2002); Doyle et al. (2003); Larsen et al. (2006); Du and Ydstie (2012); Christofides et al. (2008)).

Major bottlenecks in the design of model-based fault-tolerant control systems for particulate processes include the infinite-dimensional nature of the process model as well as the complex and uncertain dynamics of particulate processes. An effort to address these problems was initiated in El-Farra and Giridhar (2008) where a methodology for the detection and handling of control actuator faults in particulate processes was developed based on low-order models that capture the dominant process dynamics. These results were generalized in Giridhar and El-Farra (2009) to address the problems of fault isolation and robustness against model uncertainty.

A number of subsequent studies were carried out to account for various implementation issues that arise in the design of fault-tolerant control systems for particulate processes, including, for example, the discrete and delayed availability of output measurements (Napasindayao and El-Farra (2013b)), and the presence of multi-rate sampling and sensor faults (Napasindayao and El-Farra (2013a)).

In both studies, fault detection was achieved by designing a fault-free time-varying alarm threshold off-line and later comparing this with values of the residual for the entire duration of the process. However, the scheme for fault detection was stability-based, leaving "small" malfunctions that do not lead to instability to go undetected. In designing this threshold, there are competing design requirements that need to be considered. For example, there is the need to tighten the threshold for timely fault detection; however, an extremely tight bound may result in false alarms. It was also assumed in those studies that a fault identification scheme was already in place which was able to determine the nature and location of the fault. This information was utilized in determining the appropriate response for fault accommodation. After each fault, a new alarm threshold for fault detection had to be calculated and used since the closed-loop system will have different stability properties after each fault accommodation event.

In this work, our aim is to address some of these limitations by integrating within the fault-tolerant control methodology a fault identification mechanism that allows for imme-

diate detection of faults and/or malfunctions while determining its location and magnitude. One key element of the proposed scheme is that it may still be used for fault identification even after fault accommodation. This allows for timely fault detection in the event of consecutive system faults. This is an advantage over the previous detection schemes where a new alarm threshold had to be calculated after every fault accommodation event. This recalculation may result in delays in the fault detection preceding a fault. Timely or even instantaneous fault identification is important even for faults that do not immediately result in an unstable behavior since these malfunctions may later on result in poor plant performance or even instability. In addition, rapid detection will also allow for systematic scheduling of plant maintenance and equipment repair or replacement.

Motivated by the above considerations, we develop in this study a model-based framework for the integrated detection, identification and accommodation of actuator faults in sampled-data particulate processes described by complex population balance equations. Initially, model reduction techniques are applied to derive a finite-dimensional model to be used in designing a stabilizing sample-and-hold state feedback controller. This controller uses past values of the state measurements in between sampling times. The controller then utilizes updated state measurements when sensor readings are received at discrete times. Through a stability analysis, an explicit characterization of the behavior of the closed-loop system is obtained as a function of the controller design parameters, the update time, and the actuator health. This characterization is then used as a metric in determining the appropriate post-fault response once a fault is detected. Fault identification is carried out by solving a data-based moving-horizon optimization problem. Data from the fault identification scheme are used in the fault accommodation which involves modifying the controller design parameters based on the stability plots generated from the stability analysis. Finally, the proposed fault-tolerant control framework is applied to a simulated model of a non-isothermal continuous crystallizer and is shown to effectively handle simultaneous and consecutive faults.

2. MOTIVATING EXAMPLE

A well-mixed non-isothermal continuous crystallizer is used throughout the paper to illustrate the design and implementation of the model-based fault detection and accommodation to be developed. Particulate processes are characterized by the co-presence of a continuous and dispersed phase. The dispersed phase is described by a particle size distribution whose shape influences the product properties and ease of product separation. Hence, a population balance on the dispersed phase coupled with a mass balance for the continuous phase is necessary to accurately describe, analyze, and control particulate processes. Under the assumptions of spatial homogeneity, constant volume, mixed suspension, nucleation of crystals of infinitesimal size, mixed product removal, and a single internal particle coordinate—the particle size (r); a dynamic crystallizer model can be obtained from population, mass and energy balances:

$$\begin{aligned}
\frac{\partial n}{\partial t} &= \bar{k}_1(c_s-c)\frac{\partial n}{\partial r} - \frac{n}{\tau_r} + \delta(r-0)\bar{\epsilon}\bar{k}_2 e^{\left(\frac{-\bar{k}_3}{(c/c_s-1)^2}\right)} \\
\frac{dc}{dt} &= \frac{(c_0-\rho)}{\bar{\epsilon}\tau_r} + \frac{(\rho-c)}{\tau_r} + \frac{(\rho-c)}{\bar{\epsilon}}\frac{d\bar{\epsilon}}{dt} \\
\frac{dT}{dt} &= \frac{\rho_c H_c}{\rho C_p}\frac{d\bar{\epsilon}}{dt} - \frac{UA_c}{\rho C_p V}(T-T_c) + \frac{(T_0-T)}{\tau_r}
\end{aligned} \tag{1}$$

where $n(r,t)$ is the number of crystals of radius $r \in [0,\infty)$ at time t per unit volume of suspension; τ_r is the residence time; c is the solute concentration in the crystallizer; ρ is the particle density; $\bar{\epsilon} = 1 - \int_0^\infty n(r,t)\pi\frac{4}{3}r^3 dr$ is the volume of liquid per unit volume of suspension; $c_s = -3\bar{T}^2 + 38\bar{T} + 964.9$ is the concentration of the solute at saturation computed using $\bar{T} = \frac{T-273}{333-273}$; T is the crystallizer temperature; c_0 is the concentration of solute entering the crystallizer; $\bar{k}_1$, $\bar{k}_2$ and $\bar{k}_3$ are constants; and $\delta(r-0)$ is the standard Dirac function. The term containing the Dirac function accounts for the nucleation of crystals of infinitesimal size while the first term in the population balance represents the particle growth rate. The crystallizer exhibits highly oscillatory behavior due to the relative nonlinearity of the nucleation rate as compared to the growth rate. This results in process dynamics that is characterized by an unstable steady-state surrounded by a stable periodic orbit. The control objective is to suppress the oscillatory behavior of the crystallizer in the presence of actuator faults. This is carried out by stabilizing the system at the unstable steady-state which corresponds to a desired particle size distribution by manipulating the solute feed concentration (c_0) and the residence time (τ_r).

Through the method of moments, a sixth-order ordinary differential equation system is obtained to describe the temporal evolution of the first four moments of the particle size distribution, the solute concentration, and the temperature (see Chiu and Christofides (1999) for a detailed derivation). The reduced-order model can be cast in the following form:

$$\begin{aligned}
\frac{d\mu_0}{dt} &= \frac{-\mu_0}{\tau_r} + \left(1-\frac{4}{3}\pi\mu_3\right)\bar{k}_2 e^{\frac{-\bar{k}_3}{\left(\frac{c}{c_s}-1\right)^2}} e^{\frac{-E_b}{RT}} \\
\frac{d\mu_v}{dt} &= \frac{-\mu_v}{\tau_r} + v\mu_{v-1}\bar{k}_1(c-c_s)e^{\frac{-E_g}{RT}}, v=1,2,3 \\
\frac{dc}{dt} &= \frac{c_0 - c - 4\pi\bar{k}_1 e^{\frac{-E_g}{RT}}\tau_r(c-c_s)\mu_2(\rho-c)}{\tau_r\left(1-\frac{4}{3}\pi\mu_3\right)} \\
\frac{dT}{dt} &= -\frac{\rho H_c}{\rho C_p}\frac{d\mu_3}{dt} - \frac{UA_c}{\rho C_p V}(T-T_c) + \frac{(T_0-T)}{\tau_r}
\end{aligned} \tag{2}$$

For typical values of the process parameters, the global phase portrait of the system of (2) has a unique unstable equilibrium point surrounded by a stable limit cycle at $x^s = [\mu_0^s \quad \mu_1^s \quad \mu_2^s \quad \mu_3^s \quad c^s \quad T^s]^T = [0.0047 \quad 0.0020 \quad 0.0017 \quad 0.0022 \quad 992.95 \quad 298.31]^T$. Sampled measurements of the moments (μ_0, μ_1, μ_2, μ_3), the solute concentration (c), and temperature (T) are used to control the process. These state measurements are collected discretely and sent to the controller where the control action is calculated and then sent to the actuator to effect the desired change in the process state. For simplicity, we consider the problem on the basis of

the linearization of the process model around the desired steady state. The linearized process model takes the form:

$$\dot{x}(t) = Ax(t) + Bu(t) \tag{3}$$

where $x(t)$ is the vector of state variables; u is the manipulated input. The state vector is expressed as a deviation variable, $x(t) = \chi(t) - x^s$, where $\chi(t) = [\mu_0(t) \quad \mu_1(t) \quad \mu_2(t) \quad \mu_3(t) \quad c(t) \quad T(t)]^T$; and A and B the state and input Jaacobian matrices, respctively.

Over the next sections, we describe the control architecture and the fault identification scheme.

3. DATA-BASED FAULT IDENTIFICATION

3.1 Continuous and discrete fault models

To model the actuator faults, the reduced, linearized system dynamics is written in the following form:

$$\dot{x}(t) = Ax(t) + B\alpha u(t) \tag{4}$$

where $\alpha = diag\{\alpha_1, \alpha_2\}$ is a diagonal fault matrix that accounts for the presence of actuator faults or malfunctions in the system. Each of the diagonal elements in the fault matrix (α) characterizes the local health status of the individual actuators, where α_1 represents the health status of the actuator used to vary the inlet concentration (c_0), and α_2 represents the health status for the actuator used to adjust the residence time (τ_r). The entries of the fault matrix (α) take values between 0 and 1, where 0 denotes total actuator failure, while 1 denotes the fault-free state. In the absence of faults, $\alpha = I$ where I is the identity matrix. The values of α_1 and α_2 can therefore be thought of as measures of the severity of the fault, where a smaller value implies a more severe fault that reduces the effectiveness of the control actuator.

Since fault identification will be carried out using a set of discrete historical input and state measurements (collected at the sampling times), the continuous-time model in (4) needs to be converted into a discrete-time form in order to more readily compare the model predictions with the historical data. The discrete-time system takes the form:

$$x[j+1] = \widehat{A}x[j] + \widehat{B}\alpha u[j], \; j \in \{0, 1, \cdots\} \tag{5}$$

where $\widehat{A} = e^{A\Delta}$, $\widehat{B} = A^{-1}(e^{A\Delta} - I)B$, $\Delta = \tau_{j+1} - \tau_j$ is the update period which represents the time interval between discrete consecutive measurements, and j is the update instance.

3.2 Data-based fault identification

Data-based fault identification involves estimating the value of the fault parameter matrix α. This is done using past data of the state measurements and the manipulated input. These values are fitted to the faulty process model in (5) using the cost function:

$$J(\zeta_j, \hat{\alpha}) = \sum_{p=j}^{j-N_I+1} \left(\left\| x[p+1] - \widehat{A}x[p] - \widehat{B}\hat{\alpha}u[p] \right\|^2 \right) \tag{6}$$

where $\zeta_j = \{(x[j-p], u[j-p]) | p = 1, 2, \cdots, N_I\}$ denotes the past N_I historical data of the state measurements and the manipulated inputs for each jth sampling instance. Using a large value for N_I results in higher accuracy for calculated values obtained for the fault estimation matrix $\hat{\alpha}$. However, this may also result in a high computational load as well as discontinuities in the values of $\hat{\alpha}$ particularly right after a fault has occurred since the pool of I/O data used in the calculations will involve data both before and after the fault. This parameter should therefore be selected appropriately.

Using the cost function in (6), a finite-horizon least squares optimization problem can be formulated as follows:

$$\begin{aligned} \min_{\hat{\alpha}} \quad & J(\zeta_j, \hat{\alpha}) \\ \text{s.t.} \quad & 0 \leq \hat{\alpha}_i \leq 1, \;\; i \in \{1, 2\} \end{aligned} \tag{7}$$

Note that the calculated values of the fault matrix $\hat{\alpha}$ may slightly differ from the actual values of α particularly at the onset of the fault.

4. FINITE-DIMENSIONAL SAMPLED-DATA CONTROL SYSTEM DESIGN

4.1 State feedback controller synthesis

The control system design involves first synthesizing a state feedback controller that stabilizes the finite-dimensional system when the sensors continuously transmit data to the controller. We consider a state feedback controller of the form:

$$u(t) = Kx(t) \tag{8}$$

where the controller gain (K) is chosen to ensure that the eigenvalues of $A + BK$ lie in the open left-half of the complex plane.

4.2 Sampled-data controller implementation

The implementation of the controller of (8) requires continuous availability of the sensor measurements. Due to measurement sampling, the controller cannot be directly implemented since the measurements are only available at discrete time instances. To compensate for the unavailability of continuous measurements, a sample-and-hold scheme is used wherein the controller utilizes previous state measurements when current measurements are not available. At each sampling time, the corresponding values of the measured states are instantaneously transmitted to the controller and are used to update the zero-order hold model states. The model-based state feedback controller is then implemented as follows:

$$\begin{aligned} u(t) &= K\bar{x}(t), \; t \in [\tau_j, \tau_{j+1}) \\ \dot{\bar{x}}(t) &= 0, \; t \in [\tau_j, \tau_{j+1}) \\ \bar{x}(\tau_j) &= x(\tau_j), \; j \in \{0, 1, \cdots\} \end{aligned} \tag{9}$$

where $\bar{x}$ is a model state used in generating the discrete control by utilizing previously held state values $x(\tau_j)$ until the next state measurement $x(\tau_{j+1})$ becomes available, j denotes each sampling instance, and τ_j are the update

times when values of the state are collected. It should be noted that the zero-order hold model is used here only as an example for illustration purposes, and that other inter-sample model predictor schemes can be used in lieu of the zero-order hold (see, for example, Montestruque and Antsaklis (2003); Napasindayao and El-Farra (2013b)).

4.3 Closed-loop stability analysis

The objective of this section is to characterize the sampled-data closed-loop system behavior in terms of the sampling rate, Δ; the controller gain, K; and the actuator health parameter, α. This characterization will be used later in the design of the fault accommodation logic. To investigate the stability properties of the finite-dimensional sampled-data closed-loop system, we first define the model estimation error as $e = x(t) - \bar{x}(t)$, where e represents the difference between the model state given in (9) and the actual measured state. Then, defining the augmented state vector $\xi(t) = [x(t) \quad \bar{x}(t) \quad e(t)]^T$, the finite-dimensional sampled-data closed-loop system is formulated as a switched system and written in the form:

$$\begin{aligned} \dot{\xi}(t) &= F\xi(t),\ t \in [\tau_j, \tau_{j+1}) \\ e(\tau_j) &= 0,\ j \in \{0, 1, \cdots\} \end{aligned} \tag{10}$$

where F is a matrix defined as:

$$F = \begin{bmatrix} A + B\alpha K & -B\alpha K \\ A + B\alpha K & -B\alpha K \end{bmatrix}, \tag{11}$$

It can be verified (e.g., see Napasindayao and El-Farra (2013b)) that the augmented closed-loop system described by (10)-(11), subject to the initial condition $\xi(0) = [x(\tau_0)\ \bar{x}(\tau_0)\ e(\tau_0)]^T := \xi_0$, has a response of the form:

$$\xi(t) = e^{F(t-\tau_j)} N^j \xi_0 \tag{12}$$

for $t \in [\tau_j, \tau_{j+1})$, $\forall\ j \in \{0, \cdots\}$, where N is given by:

$$N = I_s e^{F\Delta} \tag{13}$$

where $I_s = diag\{I, O\}$ is a diagonal matrix that accounts for the model update at each transmission time which also resets the estimation error e to zero. The null matrix O accounts for this update. Based on (12)-(13), a necessary and sufficient condition for stability of the finite-dimensional sampled-data closed-loop system can be obtained. Specifically, consider the sampled-data closed-loop system of (9) and the augmented system of (10)-(11) whose solution is given by (12)-(13). Then the zeros solution, $\xi = [x\ \bar{x}\ e]^T = [0\ 0\ 0]^T$, is exponentially stable if and only if the spectral radius of the matrix N is less than 1, i.e., $r(N(\Delta)) < 1$. This ensures stability by limiting the growth of the closed-loop state within each update period as the measurement sampling is repeatedly executed over time.

An examination of the structure of N in (13) indicates that its spectral radius is dependent on the sampling period, Δ, and on the augmented system matrix F which, in turn, depends on the actuator health parameter, α, and the controller gain, K. All these factors are tied together through the stability condition which can, therefore, be used to examine and quantify the various interdependencies between these factors. For instance, if the sampling rate and controller gain are fixed, one can determine the level of actuator malfunction that the system can still tolerate without leading to instability. Alternatively, for a given fault, one can determine the range of controller gains or sampling periods that can be used to compensate for this fault.

5. FAULT-TOLERANT CONTROL

In this section, we use the non-isothermal continuous crystallizer example introduced in Section 2 to illustrate the proposed fault-tolerant scheme. Discrete measurements of the moments of the particle size distribution (μ_0, μ_1, μ_2, μ_3), concentration (c), and temperature (T), are used to control the system. The inter-sample state estimator is used to estimate values of the states using held values of past state measurements when actual sensor measurements are unavailable. The simulations are performed under a sampling period of $\Delta = 6$ min.

The system is controlled by simultaneously manipulating the inlet solute concentration (c_0), and the residence time (τ_r). The stability regions are obtained using the stability condition $\lambda_{\max}(N) < 1$ which is derived from the closed-loop stability analysis of the test matrix N in (13) (see Fig.1). These stability conditions were obtained as an explicit function of the controller gain (K), sampling period (Δ), and the fault parameter matrix (α).

Fig.1 depicts the stability region as a function of the health status of the actuators – with α_1 corresponding to the manipulated inlet concentration (c_0) and α_2 to that of the residence time (τ_r). The blue area enclosed by the unit contour line shows the region where the process is stable since $\lambda_{\max}(N) < 1$ (i.e., the set of faults that do not lead to instability), while the pink region denotes the set of faults that lead to instability where $\lambda_{\max}(N) > 1$. Such a plot is useful in predicting the behavior of the process and in determining the appropriate fault compensation response once a fault is identified. A partial malfunction in any of the actuators could possibly occur such that the operating point is shifted somewhere within the stability region. Such faults are not detrimental to process stability and; therefore, may not warrant immediate fault accommodation or control reconfiguration. Based on this knowledge, the plant supervisor is then able to strategically prioritize which specific control loop or plant equipment requires maintenance or replacement through this stability-based closed-loop analysis. In cases where there are more variables to consider (e.g., a larger number of manipulated variables), instead of a two-dimensional contour plot, a look-up table with values of the spectral radius of N for varying magnitudes of the process parameters may be generated off-line and then used to judge if an identified fault warrants immediate response.

Among the highlights of the data-based fault identification scheme developed in the study is the added capability of identifying partial malfunctions that do not result in system instability unlike past studies which made use of a stability-based alarm threshold. This scheme results in a more proactive approach in dealing with malfunctions instead of a reactive one which triggers action when there

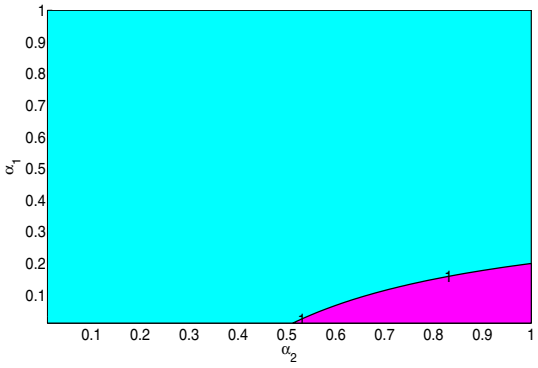

Fig. 1. Region of stability as a function of the actuators' health parameters used to determine whether fault accommodation or system reconfiguration is required ($\Delta = 6$min). Contour plot of $\lambda_{\max}(N)$ for pole values $[-1 -2 -3 -4 -5 -6]$.

is a threat of instability. Machine repair carried out at an early stage may prove to be less costly and time-consuming as opposed to the urgent repairs or fault accommodation following a more severe and destabilizing malfunction.

5.1 Fault identification under partial faults

For both the simultaneous and consecutive faults considered below, the controller gain (K) was calculated by specifying the location of the poles of $A+BK$ at $[-1\ -2\ -3\ -4\ -5\ -6]$. Fault identification was carried out using the past 10 data points ($N_I = 10$) of the state measurements and manipulated input as well as the discrete model generated in (5) to solve for the fault parameter estimation matrix ($\hat{\alpha}$) in the optimization problem in (7). Actuator faults in both manipulated variables were investigated and the simulation was carried out under a sampling period (Δ) of 6 min.

The first case involves a simultaneous fault that occurs after 10 h, with $\alpha_1 = 0.8$ and $\alpha_2 = 0.5$, where the actuator handling the inlet concentration (c_0) become 20% effective while the other actuator used in varying the residence time (τ_r) suffers a 50% loss in performance (Figs.1(a)-(b)). The second case involves a consecutive fault occurring after 5 h followed by another one at 10 h. The first fault causes a -10% step change in the performance of the actuator responsible for adjusting the residence time (τ_r) while the second fault is a gradual fault that causes a linear decline in the control action of the actuator manipulating the inlet concentration (c_0) (Fig.1(c)-(d)).

In both cases, the fault identification scheme is shown to be effective and capable of almost instantaneously locating and quantifying the faults. However, jumps in the calculated values of the fault estimation parameters were occasionally observed right after a fault had taken place. These jumps are visible even in the plot of a fault estimation parameter that was not assigned to monitor that particular actuator at fault. This behavior is attributed to the sudden disruptions in the data points used in the data-based identification method which includes values of the state and the manipulated variable before and after the fault. This is why the optimization horizon (N_I) has to be properly selected – small values result in inaccuracies in the fault identification while large values lead to sharp jumps or prolonged settling times. Due to this behavior, plant response should be suspended until the fault identification scheme settles to a final value. These sharp discontinuities; however, may provide insight on the health status of a neighboring actuator. In the case of the consecutive faults, for example, two separate faults were introduced at 5 h and 10 h. A plot of the fault estimation parameter devoted to the actuator responsible for manipulating the inlet concentration (c_0) reveals a spike at exactly 5 h when another malfunction affects the neighboring actuator (Fig.2(c)). Based on that plot alone, one can infer that a malfunction has occurred within the system.

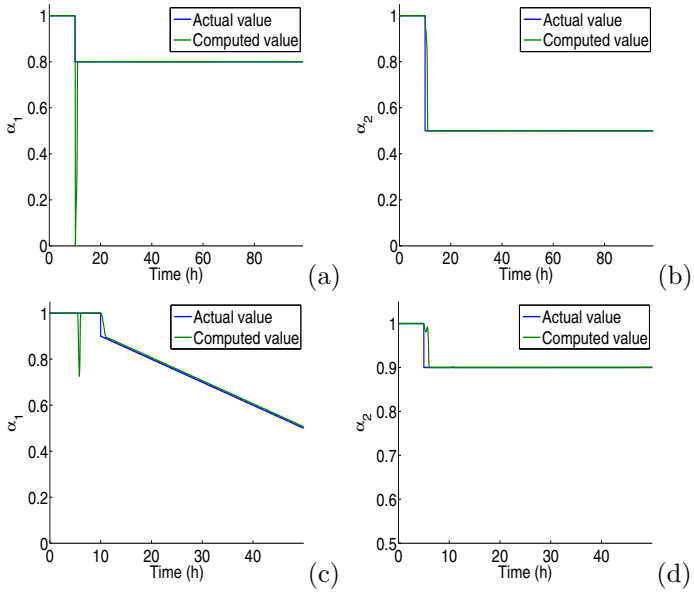

Fig. 2. Actual and calculated values of the fault estimation parameters for the manipulated inlet concentration (c_0), α_1, and the residence time (τ_r), α_2, under $\Delta = 6$ min. Plots (a)-(b): Simultaneous faults. Plots (c)-(d): Consecutive faults.

5.2 Fault identification and accommodation

To illustrate the fault accommodation capabilities of the control architecture, a destabilizing fault is introduced after 10 h of operation, causing the actuator controlling the inlet concentration (c_0) to drop its effectiveness from 100% to 45%. Initially, for the fault-free system, we select a value for the controller gain such that the poles of $A+BK$ are placed at [-9.5 -2 -3 -4 -5 -6] under a 6 min sampling period. As can be seen from Fig.3, the fault identification scheme is able to identify the location and magnitude of the fault; and it is found that the fault is in α_1. The spectral radius of N was calculated using the original parameter values and the new faulty condition, and the fault was found to be destabilizing since the new operating point was now inside the pink unstable region (Fig.4(a)). To avoid instability, fault accommodation was carried out using the stability region plot in Fig.4(a). The x-axis in the plot is based on the first pole location which is the only pole that was modified. This pole value is used as a means to calibrate the selection of the multi-dimensional

controller gain (K). The controller gain was adjusted by shifting the location of the poles of $A+BK$ to $[-6.4-2-3-4-5-6]$. This caused the operating point to return to the stable region. The closed-loop simulation profiles of the inlet outlet solute concentrations in Figs.4(b)-(c) demonstrate the destabilizing effect of the fault in the absence of fault accommodation. These undesired effects were avoided through timely fault identification and fault accommodation which maintained closed-loop stability even after a potentially disruptive fault (see Figs.4(d)-(e)).

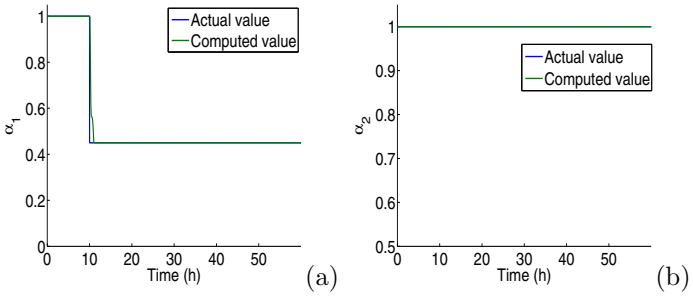

Fig. 3. Fault identification after a potentially destabilizing fault at 10 h with $\Delta = 6$ min.

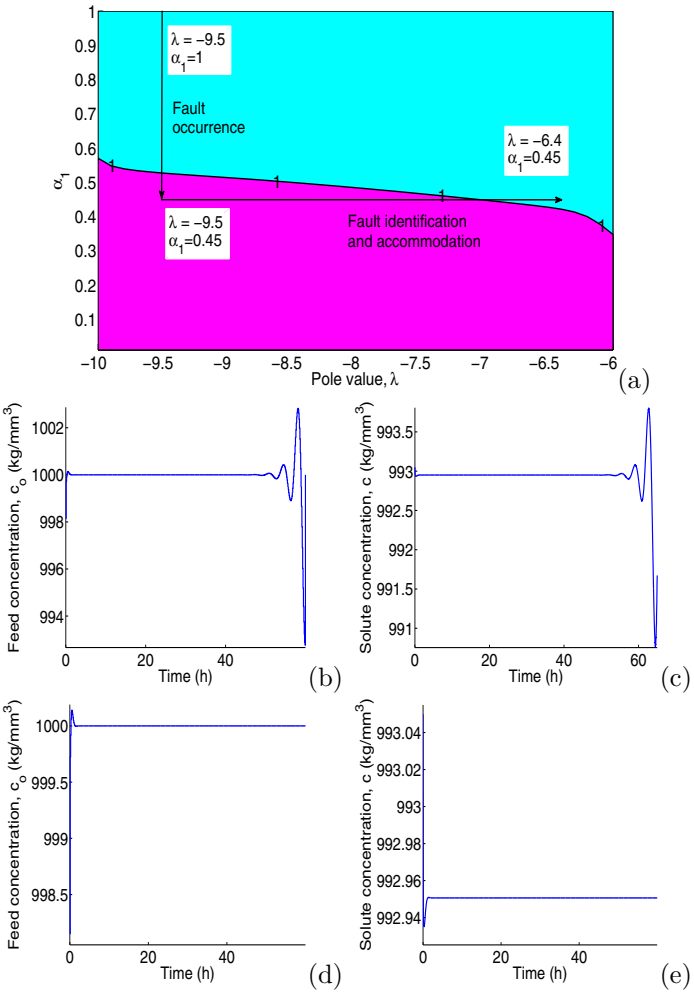

Fig. 4. Fault identification and accommodation re-establishes closed-loop stability after a potentially destabilizing fault. Plot (a): Region of stability based on the health of the actuator controlling the inlet concentration (c_0), α_1, and the pole value (λ) ($\Delta =$ 6min, $\alpha_2 = 1$). Plots (b)-(c): Closed-loop profiles of the inlet concentration (c_0) (b) and the outlet solute concentration (c) without fault accommodation. Plots (d)-(e): Closed-loop profiles of the inlet concentration (c_0) (d) and the outlet solute concentration (e) under fault accommodation.

REFERENCES

Chiu, T. and Christofides, P. (1999). Nonlinear control of particulate processes. *AIChE J.*, 45, 1279–1297.

Christofides, P.D. (2002). *Model-Based Control of Particulate Processes*. Kluwer Academic Publishers, 209 pages, Netherlands.

Christofides, P.D., El-Farra, N., Li, M., and Mhaskar, P. (2008). Model-based control of particulate processes. *Chemical Engineering Science*, 63(5), 1156 – 1172.

Doyle, F.J., Harrison, C.A., and Crowley, T.J. (2003). Hybrid model-based approach to batch-to-batch control of particle size distribution in emulsion polymerization. *Computers & Chemical Engineering*, 27(8-9), 1153–1163.

Du, J. and Ydstie, B. (2012). Modeling and control of particulate processes and application to poly-silicon production. *Chemical Engineering Science*, 67(1), 120–130.

El-Farra, N.H. and Giridhar, A. (2008). Detection and management of actuator faults in controlled particulate processes using population balance models. *Chemical Engineering Science*, 63(5), 1185 – 1204.

Giridhar, A. and El-Farra, N.H. (2009). A unified framework for detection, isolation and compensation of actuator faults in uncertain particulate processes. *Chemical Engineering Science*, 64(12), 2963 – 2977.

Hu, Q., Rohani, S., Wang, D., and Jutan, A. (2005). Optimal control of a batch cooling seeded crystallizer. *Powder Technology*, 156(2-3), 170–176.

Larsen, P., Patience, D., and Rawlings, J. (2006). Industrial crystallization process control. *Control Systems, IEEE*, 26(4), 70–80.

Montestruque, L.A. and Antsaklis, P.J. (2003). On the model-based control of networked systems. *Automatica*, 39, 1837–1843.

Napasindayao, T. and El-Farra, N.H. (2013a). Sensor fault accommodation strategies in multi-rate sampled-data control of particulate processes. In *Proceedings of the 10th IFAC Symposium on Dynamics and Control of Process Systems*, 379–384. Mumbai, India.

Napasindayao, T. and El-Farra, N.H. (2013b). Fault detection and accommodation in particulate processes with sampled and delayed measurements. *Industrial & Engineering Chemistry Research*, 52(35), 12490–12499.

Semino, D. and Ray, W.H. (1995). Control of systems described by population balance equations-II. emulsion polymerization with constrained control action. *Chemical Engineering Science*, 50, 1825–1839.